Interplay of dipolar interactions and grain-size distribution in the giant magnetoresistance of granular metals

D. Kechrakos and K. N. Trohidou
Institute of Materials Science, NCSR ''Demokritos,'' 15310 Athens, Greece
(Received 22 February 2000)

The giant magnetoresistance (GMR) of a granular metal containing interacting magnetic particles with disperse sizes and shapes is studied numerically using a tight binding Hamiltonian with spin-dependent potentials. Dipolar interactions between the magnetic particles are assumed and the equilibrium configuration of the system is obtained by a classical Monte Carlo simulation. The conductance of the system is calculated using the Kubo-Greenwood formula and real space Green function techniques. Due to the dipolar interactions acting between the grains the maximum GMR value is reduced and the saturation field is increased. When the coalescence between particles is introduced the concentration dependence of the GMR develops an optimum value close to the percolation threshold, where the effect of dipolar interactions is mostly pronounced, causing serious deviations from the predictions for noninteracting grains. Both dipolar interactions and grain size distribution are responsible for the deviations from the parabolic dependence of the GMR on the reduced magnetization at low fields. The relative importance of these two factors is investigated. Our numerical results are compared with experimental findings in Co_xCu_{1-x} granular alloys.

I. INTRODUCTION

Magnetic granular metals consist of magnetic particles (e.g., Fe, Ni, Co) with a diameter typically of a few nanometers embedded in a nonmagnetic metallic matrix (e.g., Au, Cu, Cr). The first observation of a giant magnetoresistance in granular films[1,2] motivated a great deal of experimental and theoretical effort with two main purposes. First, to reveal the underlying physical mechanisms that gives rise to the GMR effect and second, to achieve control over the physical factors that determine the size of the observed magnetoresistance. This effort is driven by the immense technological potentials of magnetic granular metals in construction of magnetic read heads combined with their relatively easy growth process (sputtering, mechanical alloying, melt spinning).

The GMR effect was first observed in magnetic Fe/Cr multilayers.[3] In particular, the multilayer exhibits high resistivity when the magnetizations of successive magnetic layers are aligned antiferromagnetically, while the resistivity drops to nearly half its value when a ferromagnetic alignment of the layers is achieved by application of an externally applied magnetic field. This effect is attributed to spin-dependent scattering of the charge carriers. Intrinsic effects (spin-polarized band structure) and extrinsic effects (magnetic or nonmagnetic impurities, lattice imperfections) both give rise to spin-dependent scattering and their relative importance remains an open question.[4] Furthermore, the direction of current, either in the magnetic planes (CIP) or perpendicular to them (CPP), produces different values for the effect. In general, the CPP arrangement produces higher GMR values than the CIP.[5]

The GMR effect in granular metals is attributed to the same physical mechanisms as in the case of magnetic multilayers, namely spin-dependent scattering of the conduction electrons off the magnetic particles.[1,2] It occurs when the size of the particles is comparable to the electronic mean free path.[2] Due to their small size, which does not exceed the correlation length for the exchange interactions, the particles consist of a single magnetic domain. When the thermal energy exceeds the magnetic anisotropy barrier the particles become superparamagnetic and in the absence of external field their magnetization vectors point in random directions. In the random configuration the system has the maximum resistivity. Application of a magnetic field aligns the magnetic moments and the resistivity of the sample drops leading to the GMR effect.

Experiments have revealed various factors that determine the size of the GMR effect. In particular, the value of GMR increases initially with increasing grain diameter and it decreases above a certain grain size. The maximum value occurs for particle diameters around the electron mean free path.[2] Varying the particle concentration, an optimum value is obtained around the percolation threshold.[6,7] Spin-dependent scattering in granular metals occurs predominantly at the magnetic-nonmagnetic interfaces of the particles with the matrix and therefore the important role of the surface structure of the particles has been underlined.[8] Finally, the choice of magnetic and nonmagnetic material for maximum GMR values remains an open issue.[9]

It was demonstrated by Xiao *et al.*[2] that the magnetoresistance data at various magnetic fields when represented as a function of the reduced sample magnetization M/M_s lie on a single curve that is very close to an inverted parabola. This dependence of the GMR on the square of the total magnetization is an indication that long range correlations between the particle moments determine the size of the effect. However, many experimental groups have observed deviations from the parabolic dependence that have been attributed to interparticle interactions,[10] to particle size distribution,[2,8] and to the coexistence of blocked and superparamagnetic particles[11] or collectively rotating and superparamagnetic particles[12] in the sample. The relative importance of these

factors in producing the deviations from the inverted parabola, is currently an open question.

The theoretical works, on the other hand, that describe the GMR effect in granular metals, include classical treatments,[13–15] semiclassical treatments based on Boltzmann's equation,[16–18] and quantum approaches based on the Kubo-Greenwood theory of conductivity.[19,20]

Two common approximations adopted in previous theoretical treatments are the following. First, that a single spin quantization axis exists in the system.[16,20] Consequently, spin-flip processes are inhibited and the two spin channels contribute to the electronic conduction in parallel. Second, that the particles are superparamagnetic and therefore, a random configuration of the magnetic moments exists at zero field. The maximum GMR effect is then obtained by comparing the conductivities of the random and the fully aligned configurations.[16,19] For superparamagnetic systems, the parabolic dependence of the GMR on the total magnetization[16,19] was proved.

Zhang and Levy[16] assumed further that a distribution of the particle sizes exists and they showed that this is responsible for the deviations from the parabolic dependence at high fields $(M/M_s \sim 1)$ in agreement with previous experiments.[2] The situation with the deviations at low fields $(M/M_s \sim 0)$ appears more complicated. The reason being that both grain-size distribution and interparticle interactions are responsible for these deviations.[8]

At room temperature, which for most granular films is greater than the blocking temperature of the isolated particles, the magnetic configuration of the system is mainly ruled by the action of the magnetostatic interactions among the particles, while the effective anisotropy energy is of secondary importance.[21] The magnetostatic interactions tend to align the magnetic moments to form flux-closure loops and thus introduce short range ferromagnetic correlations in the ensemble of particles. In magnetic multilayers, the ferromagnetic alignment of the layers produces higher conductivity values than the antiferromagnetic one. Similarly, in granular metals, the presence of ferromagnetic correlations in the ensemble leads to higher conductivity values than the fully random case. Thus the GMR effect is degraded due to the presence of magnetostatic interactions.

The resistivity of a granular metal was postulated to be proportional to the moment-moment correlation function.[22] Following this idea, certain phenomenological studies of the GMR appeared that focused on the calculation of the moment-moment correlation function[10,23,24] and demonstrated a flattening of the GMR-versus-magnetization parabola in agreement with experiments. However, in these treatments of the GMR effect, the variation of the mean free path with the particles concentration is either neglected[23,24] or treated as a fitting parameter.[10] Also a set of parameters determining the value of the resistivity are phenomenological with no clear microscopic origin.

Recently, Pogorelov *et al.*[18] extended the transport model of Zhang and Levy[16] by allowing for coherent scattering of the carriers by neighboring magnetic particles. They showed that, short range magnetic correlations enter the final expression for the magnetoresistance and cause mixing of the majority and minority transport channels. However, no numerical predictions are made in this work, because an expression for the moment-moment correlation function is lacking. Furthermore, this model[18] is developed in the dilute limit and its applicability to dense systems is debatable. Dense systems are desirable as the GMR effect appears to grow with particle concentration and maximum values appear around the percolation limit.[6,7]

We believe that a theoretical transport study of the GMR in granular metals that includes a realistic description of the magnetic structure is currently missing from the literature. This study is important in order to understand the observed deviations of the experimental results from the predictions of the existing theoretical models.

We have recently presented preliminary results of a numerical study of the GMR in a granular metal, where the magnetic correlations, arising from magnetostatic interactions between the particles, were included in the calculation of the conductivity.[25] Our method is a combination of the real space Kubo-Greenwood formula for the conductivity of a system described by a tight binding Hamiltonian with the Monte Carlo simulation technique. The implementation of the Kubo-Greenwood formula for a tight-binding Hamiltonian constitutes a very efficient and reliable method to study spin-dependent transport in nanoscale magnetic structures. It has been previously used to study the magnetoresistance[26] and the thermopower[27] in magnetic multilayers and the magnetoresistance in granular alloys.[19,28] The Monte Carlo simulation is a well established technique[32] that reproduces the micromagnetic configuration of interacting magnetic systems at finite temperatures. Our approach has, on one hand, the advantage of the phenomenological models in providing a realistic description of the micromagnetic state[10,23,24] and, on the other hand, the advantage of the quantum-mechanical treatment of electronic transport in including multiple scattering effects. The latter are of particular importance in dense samples.

As the concentration of magnetic particles in a granular alloy increases, the coalescence between neighboring particles is an inevitable phenomenon. Coalescence causes formation of clusters of particles with a distribution of sizes and shapes. It also manifests itself in the concentration dependence of various macroscopic quantities. For example, the coercive field and the magnetoresistance[6,7] of the sample develop a characteristic peak at concentrations around the percolation threshold. To our knowledge, the role of coalescence has been neglected in all previous models of the GMR in granular alloys, a fact that limits their applicability to very dilute systems. In the present work, we study the GMR effect in the whole concentration range and include the effect of particle coalescence by a percolation model,[29] which is valid when the thermally driven diffusion of magnetic particles is negligible. According to the percolation model the particles occupy random sites in space and the various cluster sizes are generated by a cluster counting algorithm performed on this random system.[29] There are two reasons for choosing this model to describe the morphology of the granular system.

First, with the recently developed technique of low-energy cluster beam epitaxy,[6,30] magnetic clusters are formed in flight and are mass selected before they are co-deposited on a substrate with the atoms of the nonmagnetic matrix. With this technique extremely narrow size distributions of

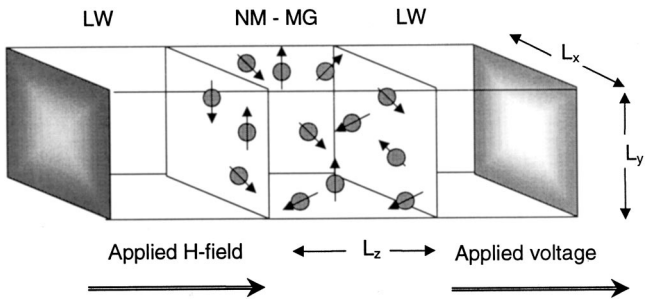

FIG. 1. Sketch of the geometry used to calculate the conductivity of the granular alloy.

particles are produced and particle coalescence after deposition is the major mechanism that leads to formation of larger clusters. Our percolation model describes satisfactorily this situation and predicts, at least qualitatively, the correct concentration dependence of the magnetoresistance.

Second, the magnetic properties and GMR of granular alloys, that are prepared by thermal annealing, are commonly analyzed by fitting the grain-size distribution function to a log-normal function.[8] The cluster size distribution generated by the percolation algorithm[29] for concentrations below the percolation threshold shares the same essential features with the log-normal distribution, as for example, the long tail and the dependence of standard deviation on the mean value. We therefore anticipate that this model can reveal the interplay of size distribution and interaction effects that occur in dilute granular systems.

This work is organized as follows. In Sec. II we introduce the spin-dependent tight binding Hamiltonian that describes the electronic structure of the granular metal and gives the corresponding Kubo-Greenwood expression for the conductivity. The use of a localized spin-dependent potential is justified as long as the electronic mean-free path ($l \sim 10^2$ Å) in granular metals is larger than the size of the granules ($D \sim 10$ Å) and therefore the magnetic particle scatters as a whole.[18,19] The Monte Carlo method used to obtain the magnetic structure and the thermal average of the conductivity is also presented in the same section. In Sec. III we present and discuss the numerical results for systems containing well separated particles (monodisperse) and systems containing clusters of coalesced particles (polydisperse). Finally, in Sec. IV we summarize the main conclusions.

II. MICROSCOPIC MODEL OF MAGNETORESISTANCE

We consider a finite sample of a granular system with two semi-infinite electrodes attached to opposite sides, as shown in Fig. 1. We describe the electronic structure of the composite system by the following single band tight binding Hamiltonian on a simple cubic lattice:[19]

$$H=\sum_{i,\alpha}\varepsilon_i c_{i\alpha}^{+}c_{i\alpha}+t\sum_{\langle i,j\rangle,\alpha}c_{i\alpha}^{+}c_{j\alpha}-J\sum_{\substack{i\in MG\\ \alpha,\beta}}c_{i\alpha}^{+}(\hat{m}_i\cdot\hat{\sigma})_{\alpha\beta}c_{i\beta}. \tag{1}$$

Here i,j are the site labels, $c_{i\alpha}^{+}(c_{i\alpha})$ is the creation (annihilation) operator of an electron with spin α at site i, ε_i is the atomic potential on site i and it takes the values $\varepsilon_{\mathrm{LW}}$ in the electrodes, $\varepsilon_{\mathrm{NM}}$ in the nonmagnetic matrix, and $\varepsilon_{\mathrm{MG}}$ on the magnetic sites. t is the hopping integral between nearest neighbors $\langle i,j\rangle$ and is fixed throughout the whole structure. J is the exchange potential on the magnetic sites and $\sigma_x,\sigma_y,\sigma_z$ are the Pauli matrices. The third term in Eq. (1) is the spin-dependent scattering potential that causes the GMR effect. The energy parameters in Eq. (1) are measured in units of the hopping integral. The strength of the spin-dependent potential, in Eq. (1), is proportional to the cosine of the angle between the electronic spin $\hat{\sigma}$ and the local magnetization axis $\hat{m}_i$. When the applied magnetic field is not strong enough to saturate the sample, there is no unique magnetization axis in the system and therefore the spin-dependent term in Eq. (1) causes mixing of the spin-up and spin-down states and introduces an elastic spin-flip scattering mechanism in the electronic transport.

We mention that the internal magnetic structure of the particles is neglected within our model. This approximation is justified, because even room temperature, at which most measurements are taken, is well below the Curie temperature of Fe or Co or Ni, and the magnetic particles are, to a good approximation, saturated.

Notice also that in Eq. (1) we use a single band to describe the electronic structure of the system. Thus the *s-d* hybridization for the transition metal is neglected. As previous studies have demonstrated,[28] inclusion of the *s-d* hybridization in the calculation leads to slightly different GMR values but it does not change the essential features of the GMR effect, as, for example, the variation with the size of magnetic particles or the concentration. We therefore expect that this simplification serves the purpose of the present work, which is to demonstrate the interplay of grain size distribution and dipolar interaction effects.

We describe the composite system electrode-sample-electrode as a sequence of layers containing L_xL_y sites (atoms) each. The corresponding Green function is defined as

$$G_{\alpha\beta}^{(\pm)}(k,k')=\left\langle k,\alpha\left|\frac{1}{E_F-H\pm i\eta}\right|k',\beta\right\rangle, \tag{2}$$

where k is the layer index, E_F is the Fermi energy and η is an infinitesimally small positive number. Notice that in general the Green function is nondiagonal in the spin indices α,β. The zero-temperature conductance in the Kubo-Greenwood formalism and for the Hamiltonian in Eq. (1) reads[19]

$$\Gamma=\frac{2e^2t^2}{h}\mathrm{Tr}\left(\begin{array}{c}\tilde{G}(k,k)\tilde{G}(k-1,k-1)+\tilde{G}(k-1,k-1)\tilde{G}(k,k)-\\ \tilde{G}(k,k-1)\tilde{G}(k-1,k)-\tilde{G}(k-1,k)\tilde{G}(k,k-1)\end{array}\right) \tag{3}$$

with

$$\tilde{G}(k,k')=\frac{1}{2i}[G^{(-)}(k,k')-G^{(+)}(k,k')]. \tag{4}$$

We compute the Green function for the composite system electrode-sample-electrode using a real space recursion method.[19] First, the Green function at the surface layer of a semi-infinite cubic lattice with a $L_x \times L_y$ surface supercell $G_s(0,0)$, that describes the (left) electrode, is obtained by means of a transfer matrix scheme.[31] Next, the successive layers of the granular film are attached to the free surface of the left electrode and the corresponding Green function of the outermost layer k is obtained using Dyson's equation

$$G(k,k)=[P(k,k)^{-1}-U(k,k-1) \times G(k-1,k-1)\cdot U(k-1,k)]^{-1} \tag{5}$$

with $U(k,k')$ the interlayer coupling matrix and $P(k,k)=[E_F-H(k,k)+in]^{-1}$ the intralayer Green function of the kth granular layer. In the final step, after the L_z-th layer is added, the surface of the right electrode is attached, using Eq. (5) but with $P(k,k)$ replaced by the surface Green function of the cubic lattice on the free surface layer $G_s(0,0)$. The Green functions in Eqs. (3)–(5) are $2L_xL_y \times 2L_xL_y$ matrices and the trace in Eq. (3) is over the spin indices α,β and all sites in the two planes k,k'.

It is evident from Eq. (1) that a particular configuration of the magnetic moments introduces a distribution of local potentials into the sample that in turn determines the sample resistance. The positions of the magnetic particles in a granular metal are random. We, therefore assume that the spin-dependent potentials in Eq. (1), are located at random sites on the lattice. However, the strengths of the local potentials are determined by the orientation of the local magnetic moments, which are correlated due to interparticle interactions. In thermodynamic equilibrium, the magnetic configuration is such that the total energy of the assembly is at a global minimum. To obtain the energy minimum we proceed as follows. We describe the magnetic granular system by an assembly of identical three dimensional classical spins (magnetic moments) located at random on the sites of a simple cubic lattice. The spins interact via dipolar magnetostatic forces. The total energy of the system reads

$$E=\sum_i \left[g\sum_j \frac{\hat{m}_i\cdot\hat{m}_j-3(\hat{m}_i\cdot\hat{R}_{ij})(\hat{m}_j\cdot\hat{R}_{ij})}{R_{ij}^3}-h(\hat{m}_i\cdot\hat{H})\right], \tag{6}$$

where m_i is the magnetic moment (spin) of ith particle, g is the dipolar strength, h is the Zeeman energy, and R_{ij} is the distance between particles i and j. Hats indicate unit vectors. The energy parameters in Eq. (6) are measured in arbitrary units, while distances are measured in units of the particle diameter D. In a previous study,[21] we have shown that for temperatures above the blocking temperature of the isolated particles and for a wide range of particle concentrations (up to ~ 0.8) the interparticle dipolar interactions have a ferromagnetic character. In this regime, the single-particle anisotropy is immaterial, to a first approximation, so we have omitted the corresponding terms in Eq. (5).

The equilibrium spin configuration is obtained from minimization of the total energy of the system using the Monte Carlo technique and the Metropolis algorithm.[32] According to this algorithm a particle is chosen at random, a move of its spin is considered and the change in the energy of the system (ΔE) is calculated. If $\Delta E \leqslant 0$, the transition to the new state is made and the new configuration is accepted. If $\Delta E > 0$, the transition to the new state and the acceptance of the configuration are made with probability equal to $\exp(-\Delta E/k_BT)$. The step of change of the spin direction is adjusted so that approximately 50% of the attempted moves are successful.[32] Thermal averages of the macroscopic quantities of interest are obtained from simple arithmetic averages over the accepted configurations. In particular, the conductivity for each accepted configuration is calculated using Eqs. (1)–(5), and the (reduced) magnetization M/M_s is equal to the average value of the component of the spin along the field axis.

Dipolar interactions introduce an extra anisotropy to the system and consequently the assembly of dipolar interacting particle develops hysteretic behavior. One should therefore distinguish between the anhysteretic and the hysteretic dependence of the magnetization or the conductivity on the external field. To model the anhysteretic behavior of the system, the simulation starts with a random initial magnetic configuration that describes a demagnetized sample and an external positive (or negative) field is applied. For the hysteretic behavior, the simulation starts with a fully saturated assembly along the negative (or positive) z axis and a negative (or positive) external field is applied along the same axis. During the simulation, the required long range part of the dipolar interaction energy is calculated using the Ewald summation technique.

For a given sample, the field-dependent magnetoresistance (MR) is defined with respect to the minimum resistance as $\mathrm{MR}(H)=[R(H)-R_s]/R_s \times 100$, where the field-dependent resistance is defined as $R(H)=1/\Gamma(H)$ and R_s is the resistance of a fully saturated sample.[33] We adopt this definition of the magnetoresistance, because in the saturated state the micromagnetic configuration of the system is unique and so the minimum resistance of the sample has a well defined value. Also, from the computational point of view, the value of R_s is obtained without implementing the Monte Carlo simulation, because the micromagnetic configuration at saturation is known. Therefore, our results for MR do not depend on the maximum applied field used.

The calculation of the thermodynamic quantities (magnetization, conductivity, and magnetoresistance) is repeated for a set of different samples with random positions of magnetic particles and eventually the configurational average is obtained by taking the arithmetic average of the results for all samples.

III. NUMERICAL RESULTS AND DISCUSSION

In order to proceed with the numerical results we make the following choice for the parameters of our model. As mentioned earlier the hopping integral is constant throughout the electrodes and the granular sample and it defines the energy unit ($t=1.0$). Therefore the bandwidth in all materials (electrode, matrix, magnetic grain) is $W=12$. The on-site potentials in the electrodes ($\varepsilon_{\mathrm{LW}}$) and in the nonmagnetic

matrix (ε_{NM}) are equal, $\varepsilon_{LW}=\varepsilon_{NM}=0$, so that the electrode-sample contact does not introduce any contact resistance. On the magnetic sites we choose $\varepsilon_{MG}=+2$ and $J=+2.0$, so that the electrons in the majority spin band are less scattered at the magnetic grains than those in the minority band, when the magnetic moments of the grains are aligned ferromagnetically. This choice of parameters introduces in our model the essential aspect of asymmetry in spin-dependent scattering that has been observed in Co/Cu magnetic multilayers and that is expected to be valid for granular CoCu alloys.[28] The Fermi level is at the band center ($E_F=0$) and consequently the conduction electrons have a wavelength comparable to the grain size ($\lambda_F=D$). An infinitesimal broadening parameter $n=0.1$ is used for the calculation of the Green function transfer matrices, that leads to convergence after a small number of iterations ($N\approx 7$) and zero broadening is used in the recursion scheme of Eq. (5).

The energy parameters that determine the micromagnetic configuration are related to the actual grain parameters as $g=m^2/D^3$ and $h=mH$, where $m=M_sV$ is the magnetic moment of the grains. For Co particles with mean diameter $D=60$ Å and saturation magnetization $M_s=1400$ emu/cm^3, we obtain $g=1.14\times 10^{-13}$ erg and therefore the ratio $k_BT/g=0.36$, at room temperature ($T=300$ K), and $k_BT/g=0.01$, at low temperature ($T=8.2$ K). Also the ratio $h/g=1$ corresponds to a field of $H=0.73$ kOe. These results indicate the appropriate range of values for the energy parameters (k_BT,g,h) that enter the Monte Carlo simulations.

In our simulations, a finite granular sample with dimensions $L_x=L_y=L_z=10$ and periodic boundary conditions is considered. This contains approximately 100 up to 700 spins, depending on the concentration value. Equilibrium is reached after 10^4 Monte Carlo steps per spin (MCSS). Further increase of the number of MCSS by an order of magnitude does not modify substantially our results for the magnetization and the conductivity. At every field value, the first 10^3 MCSS are not included in the statistical averages in order to allow for relaxation towards the equilibrium state. Configurational averages are performed over 10–15 random samples. In what follows, first we discuss the results for monodisperse systems containing identical Co particles and second the results for polydisperse systems arising from coalescence of Co monomers.

A. Monodisperse samples

We show in Fig. 2 the hysteresis loop curves for a granular system with concentration $p=30\%$ of Co particles and in Fig. 3 the anhysteretic magnetization curve for the same system. This value of the concentration corresponds to a metal volume fraction of $x_v\sim 16\%$, because in a rigid sphere model on a cubic lattice one has the relation $x_v=(\pi/6)p$. Thus the results in Figs. 2 and 3 correspond approximately to the system $Co_{16}Cu_{84}$. The magnetization data for the noninteracting assembly follow the well known Langevin dependence on the applied field. The presence of dipolar intergranular interactions introduces anisotropy in the system and the assembly of dipolar particles develops hysteresis with a remanence magnetization $M_R\sim 20\%$ and $H_c\sim 0.15$ kOe at $T=82$ K. The assembly with noninteracting grains has a saturation field $H_s\sim 1.5$ kOe, which is increased to H_s

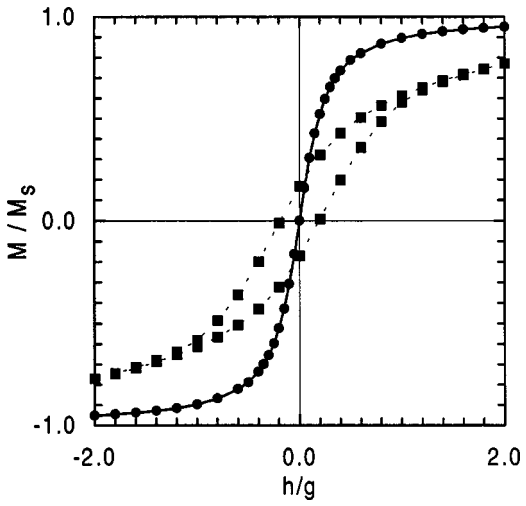

FIG. 2. Hysteresis loop for a dipolar system (squares) and magnetization curve for a noninteracting system (circles). Parameters $p=30\%$ ($Co_{16}Cu_{84}$) and $T=82$ K. Monodisperse samples.

~ 3.0 kOe (not shown in Figs. 2 and 3) due to dipolar interactions. A decrease of the initial susceptibility due to the presence of dipolar interactions is also observed (Fig. 3), from the value $x_0\sim 9.3$ emu/Oe cm^3 for the noninteracting systems to the value $x_0\sim 1.6$ emu/Oe cm^3 for the dipolar one. The increase of the saturation field and the decrease of the initial susceptibility observed in the dipolar system relative to the noninteracting one, reflect the fact that dipolar interactions among the particles inhibit the alignment of their magnetic moments along the external field axis.

The field dependence of the hysteretic MR is shown in Fig. 4 and that of the anhysteretic MR in Fig. 5. Notice that the maximum of the hysteretic MR appears at the coercive field and not the zero field, in agreement with experiments.[2] By comparison of the noninteracting and the dipolar systems we deduce that due to dipolar interactions, both the maximum MR value and the sensitivity of the MR to the external field are reduced. The reduction of the maximum MR value

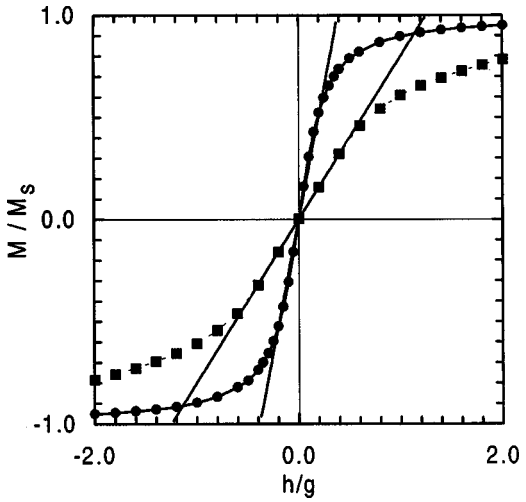

FIG. 3. Anhysteretic magnetization curve for a dipolar system (squares) and magnetization curve for a noninteracting system (circles). Straight line fits to the low-field data are shown. Parameters $p=30\%$($Co_{16}Cu_{84}$) and $T=82$ K. Monodisperse samples.

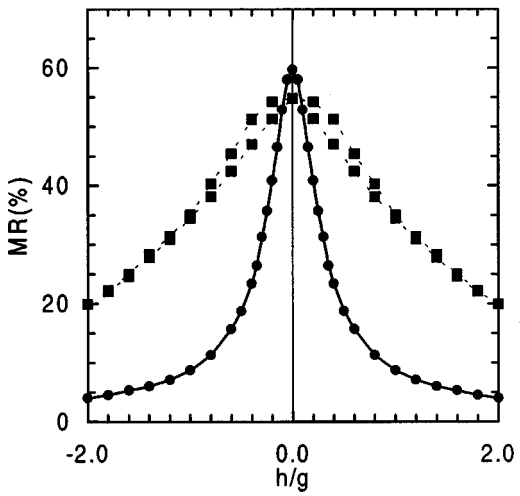

FIG. 4. Field dependence of hysteretic magnetoresistance for a dipolar sample (squares) and for a noninteracting sample (circles). Parameters: $p=30\%$ ($Co_{16}Cu_{84}$) and $T=82$ K. Monodisperse samples.

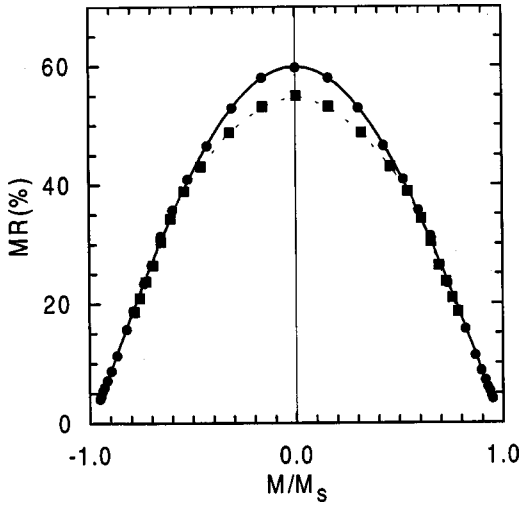

FIG. 6. Anhysteretic magnetoresistance versus reduced sample magnetization for a dipolar sample (squares) and for a noninteracting sample (circles). Parameters: $p=30\%$ ($Co_{16}Cu_{84}$) and $T=82$ K. Monodisperse samples.

indicates that the zero field configuration is not random, but positive (ferromagnetic) moment correlations develop in the assembly of particles. Thus the difference between the zero field and high field resistivities is reduced. Maximum randomization of the magnetic moments occurs at the coercive field, which explains the peak of the hysteretic MR at H_C. Notice also that the MR curve for the dipolar system is more rounded around the zero field than the corresponding curve for the noninteracting system. This behavior is related to the difficulty of a weak external field to rotate the magnetic moments that are coupled via dipolar forces. The same physical situation manifested itself in the reduction of the initial susceptibility (Fig. 3).

The maximum MR value shown in Figs. 4 and 5 is MR $\sim 55\%$. In the definition of the magnetoresistance with respect to the zero field resistance, the maximum value is $MR'_{max}=(R_S-R_0)/R_0\times 100$. This result is related to ours by $MR'_{max}=-MR_{max}\times(R_S/R_0)$. For the data shown in Figs. 4 and 5 the relevant ratio is found $R_S/R_0\sim 0.6$, which provides $MR'_{max}\sim -35\%$. Experiments on granular films containing Co particles[2,6,10] report values of MR′ in the range of -10–$-20\,\%$. We demonstrate below that our overestimation is improved by inclusion of the size distribution in our model.

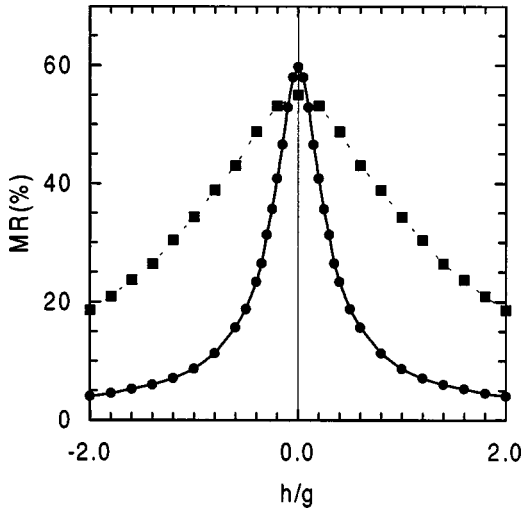

FIG. 5. Field dependence of anhysteretic magnetoresistance for a dipolar sample (squares) and for a noninteracting sample (circles). Parameters: $p=30\%$ ($Co_{16}Cu_{84}$) and $T=82$ K. Monodisperse samples.

In Fig. 6 we plot the ahnysteretic magnetoresistance as a function of the reduced magnetization of the system. For the noninteracting system, the parabolic dependence $MR=c(1-M^2)$ is obtained in agreement with previous experimental[2] and theoretical[16–19] studies. A small flattening of the parabola (-8%) is observed near the zero field due to dipolar interactions. These deviations away from the parabola at low fields have been previously observed in experiments and they have been mainly attributed to interaction effects among the grains[10] or to grain-size distribution.[8]

Previous Monte Carlo simulations[23,24] have also predicted a small flattening ($\sim 10\%$) of the moment-moment correlation function close to zero field and supported the role of the dipolar interactions in determining this flattening. However, both the deviations shown in Fig. 6 and the ones previously calculated[23,24] are much smaller than the ones measured in recent experiments ($\sim 50\%$).[10] We show below that size distribution effects improve this discrepancy.

In Fig. 7 we show the concentration dependence of the (maximum) resistance and magnetoresistance for a monodisperse system. The scattering potentials for the conduction electrons are small compared to the bandwidth W, $\epsilon_{NM}-\epsilon_{MG}\pm J\ll W$, consequently, the resistance of the sample increases almost linearly with concentration below the percolation threshold ($p_c\sim 0.3$). The MR also increases with concentration because more spin-dependent scatters exist in the system. The MR exhibits a concave parabolic dependence on the concentration. It was recently shown[18] that the concave shape in the concentration dependence of the MR is an indication of important background spin-independent scattering in the sample. In our model spin-independent scattering is provided by the boundaries of the sample. Notice, finally, in Fig. 7 that the deviations between the noninteract-

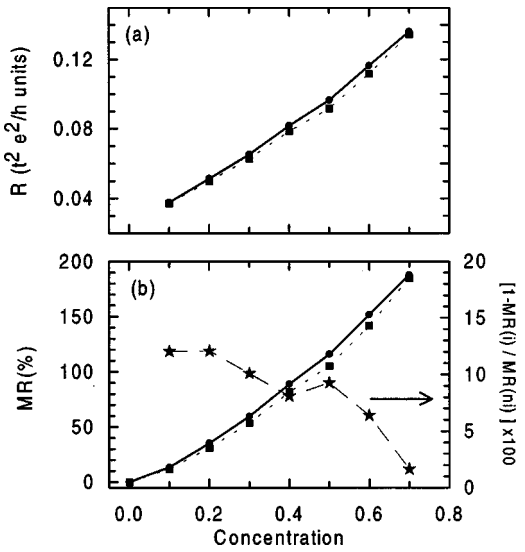

FIG. 7. Concentration dependence of (a) the zero-field resistance and (b) the zero-field magnetoresistance of dipolar (squares) and noninteracting (circles) monodisperse Co_xCu_{1-x} samples. The percentage change of the MR due to dipolar interactions is also shown (stars) and MR(ni), MR(i) denote the MR values for the noninteracting and interacting systems, respectively. Parameters: $T=8$ K.

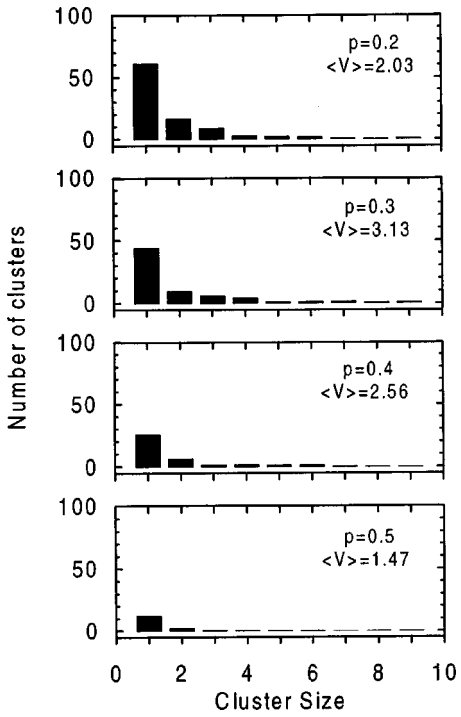

FIG. 8. Distribution of magnetic cluster size at various concentrations. Above $p=0.3$ an infinite (percolation) cluster is formed that is not shown in the histograms.

ing and the dipolar system are larger below the percolation threshold and they tend to zero at high concentrations ($p \sim 0.8$). At large concentrations, the details of the underlying auxiliary lattice become important and in particular the sc lattice, that is used in our study, when fully occupied by dipolar particles is known to lead to a columnar antiferromagnetic ground state.[34] For this type of ordering of the dipoles, the moment-moment correlation function is zero, when averaged over the two ferromagnetic sublattices, and the resistance of the system is very close to its value in the case of a random configuration. Thus it appears that in the dense limit the dipolar interactions do not modify the MR.

The structural model used so far, assumes the presence of well separated magnetic particles in the granular alloy and emphasizes the role of dipolar interactions alone. It reproduces qualitatively certain features of the experiments, as the flattening at low fields of the MR versus magnetization parabola, the reduction of the maximum GMR effect and the reduction of the sensitivity of the GMR effect on the applied field. But, it wrongly predicts a continuous increase of the MR with particle concentration. The concentration dependence of the MR obtained in recent experiments[6,7] shows an optimum value around the percolation threshold. Therefore, the applicability of the model with well separated particles is restricted to dilute systems only. To proceed with more dense samples, we take account of the coalescence between granules. This effect leads to formation of clusters of various sizes and shapes and eventually the granular system becomes polydisperse.

B. The percolation model and polydisperse samples

We describe the effect of grain coalescence by the following percolation model. The grains (monomers) are distributed at random with a certain probability p on the sites of a simple cubic lattice. Then a cluster counting algorithm[29] is implemented that groups the monomers into clusters according to the rule that nearest-neighbor monomers belong to the same cluster. This structural model produces a distribution of cluster sizes that is shown in Fig. 8 for various concentrations. Notice that the distribution is highly asymmetric and monomers are the most frequently appearing clusters in the sample. Around the percolation threshold ($p_c \sim 0.3$), the tail of the distribution is extremely long indicating that clusters of all sizes exist in the system. The average cluster size varies with the concentration p (Fig. 9) and the maximum average size appears close to the percolation threshold. Above this threshold, a cluster that spans the sample (infinite cluster) exists and the rest of the particles tend to form clusters of gradually decreasing size.

Regarding the magnetic structure of the clusters, we assume for simplicity that within each cluster the magnetic

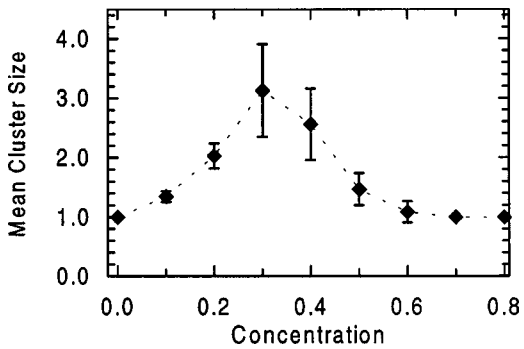

FIG. 9. Variation of the mean cluster size with concentration of magnetic particles. Error bars indicate the dispersion of cluster sizes at each concentration. The infinite (percolation) cluster is not included in the statistics.

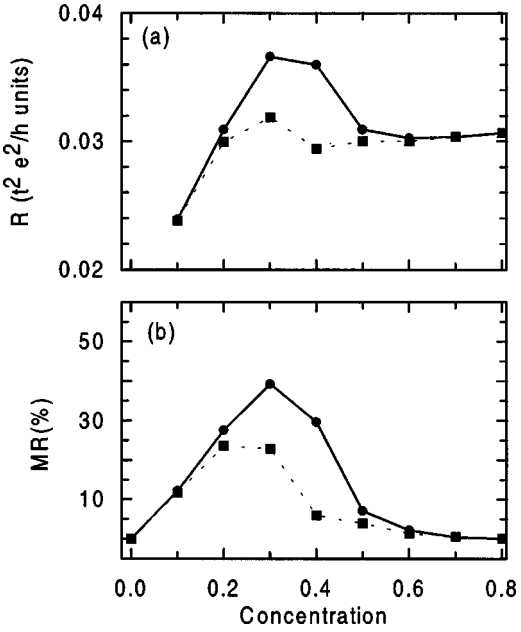

FIG. 10. Concentration dependence of (a) the zero-field resistance and (b) the zero-field magnetoresistance of dipolar (squares) and noninteracting (circles) Co_xCu_{1-x} samples. Coalescence is allowed in all samples. Parameters: $T=82$ K.

moments of the monomers rotate in cohesion. In other words, multidomain formation is not allowed, not even in the infinite cluster that represents the bulk material. This is a reasonable approximation provided that spin-dependent scattering at domain walls and anisotropic magnetoresistance are not considered in the present study. The magnetostatic energy of the system is expressed as a sum of terms corresponding to the dipolar energy of pairs of monomers belonging to different clusters.

The concentration dependence of the zero-field resistance and the maximum magnetoresistance of a system with coalescence is shown in Fig. 10. Notice that the characteristic peak around the percolation threshold appears and that the overall shape of the MR curve is in satisfactory agreement with the experimental measurements.[6,7] The increase of both R and MR below the percolation threshold is attributed to the gradually increasing number of spin-dependent scatterers (Co monomers) in the sample. Well above the percolation threshold ($p>0.5$) the infinite cluster occupies almost the whole volume of the sample and the resistance is approximately equal to the bulk resistance of Co. In the same regime, the MR tends to zero, because the electrons in the sample travel through a single magnetic domain that is formed by the infinite Co cluster. In other words, the peak in MR is the result of competition between two factors, namely, the increasing number of spin-dependent scatterers that causes an increase of MR (see Fig. 7) and the increasing mean cluster size that leads to a decrease of MR.

Even below the percolation threshold, coalescence occurs to a certain extend and the average cluster size is greater than a monomer. This increase of the average cluster size is responsible for the reduced MR values observed in systems with coalescence compared to the values in systems containing well separated particles with the same concentration of magnetic material. This is demonstrated by comparison of the MR data below the percolation threshold in Figs. 7 and 10.

In addition to cluster size effects, further decrease of the MR value is caused by dipolar interactions. We can see in Fig. 10 that the reduction of MR due to dipolar interactions is more dramatic now, compared to the monodisperse system (Fig. 7). The largest deviations between the noninteracting and the dipolar systems are observed right above the percolation threshold ($p\sim0.4$). The reason is that due to the formation of large clusters, strong local fields act on the smaller clusters and produce ordering of their magnetic moments. This ordering of the smaller clusters due to the fields of the few large clusters leads to strongly reduced MR values at concentrations above the percolation threshold ($p=0.3$–0.4). For example, the noninteracting system exhibits a substantial MR value ($\sim30\%$) at $p=0.4$, while the dipolar system, at the same concentration, shows a very weak MR effect ($\sim5\%$).

If the MR is defined with respect to the maximum (saturation) resistance, the MR values at $p=0.3$ ($Co_{16}Cu_{84}$) are $MR'=-22\%$ for the noninteracting system and $MR'=-19\%$ for the dipolar system. These results should be compared with the experiments of Xiao *et al.*[2] who report values of $MR'=-10$–$20\,\%$ for $Co_{20}Cu_{80}$ samples annealed at various temperatures and of Parent *et al.*[6] who report maximum MR values $MR'=-10$–$15\,\%$ for $Co_{25}Ag_{75}$ samples grown by cluster beam epitaxy. We believe that there is a reasonable agreement with these experiments, given the simplicity of our model for the electronic structure and the magnetic structure of the granules.

The size distribution in a granular film that has been thermally annealed is commonly fitted to a log-normal function.[8] The size distribution function produced by the percolation model (Fig. 8) shares the same essential features with the log-normal function, namely, the long tail and the dependence of the mean value on the standard deviation. Therefore, the percolation model serves also as a structural model to study the interplay of size distribution and interaction effects in granular films.

We show in Fig. 11 the anhysteretic magnetization curve for a system with $p=0.3$, that contains the distribution of Co clusters shown in Fig. 8. The mean cluster size is increased relative to the monodisperse sample $\langle V\rangle\sim3$ and consequently, saturation is achieved at lower fields $H_S\sim0.45$ kOe for the noninteracting sample and $H_S\sim1.5$ kOe for the dipolar sample. The field dependent MR is plotted in Fig. 12. It is important to notice that in this system a drastic reduction ($\sim25\%$) of the maximum MR value is observed due to dipolar interactions. The corresponding reduction for the monodisperse system ($V=1$) was only $\sim8\%$ (Fig. 5).

In recent measurements of MR in CoCu polydisperse granular samples, Allia *et al.*[10] observed large reductions (~10–$70\,\%$) in their MR data with respect to the theory for noninteracting particles. Our results in Fig. 12 indicate that similarly large reductions are predicted within a transport calculation that takes into account both the cluster size distribution and the interaction effects among the clusters. The large reductions of the MR values is the combined effect of these two factors. In Fig. 13, we demonstrate the effect each of these factors independently has on the MR value and also their combined effect. We plot the MR data versus the square

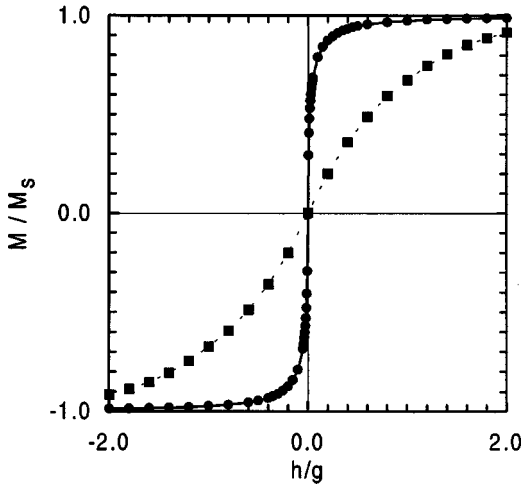

FIG. 11. Anhysteretic magnetization curve for a dipolar system (squares) and magnetization curve for a noninteracting system (circles). Parameters $p=30\%$ ($Co_{16}Cu_{84}$) and $T=82$ K. Coalescence is allowed in both systems.

of the sample magnetization for four different samples with the same concentration of magnetic material ($p=0.3$) and the same average cluster size. In particular, we show results for a monodisperse noninteracting system with $V=3$, a polydisperse noninteracting system with $\langle V\rangle\sim 3$, a monodisperse dipolar system with $V=3$ and a polydisperse dipolar system with $\langle V\rangle\sim 3$. Making this choice, the average cluster size and the metal volume fraction are approximately the same in all systems, while the width of the size distribution is allowed to take the zero value, in the case of the monodisperse system, and a large value in the case of the polydisperse system (see Fig. 9).

Consider first the overall arrangement of the curves. In a polydisperse noninteracting sample, the presence of clusters with size smaller than the mean size leads to increased MR values relative to the monodisperse sample. This happens because the GMR effect decreases with increasing cluster size.[2,16,19] When the interactions among the clusters are

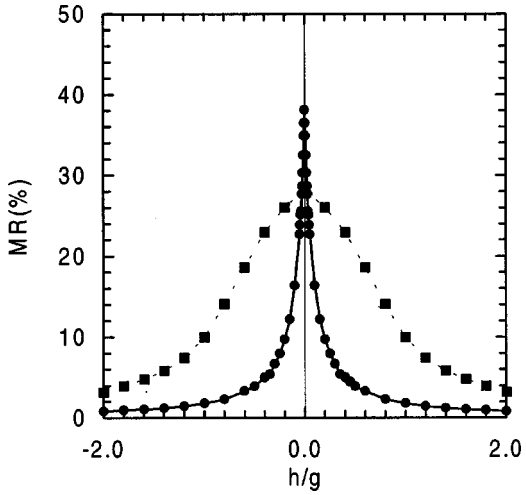

FIG. 12. Field dependence of anhysteretic magnetoresistance of a dipolar sample (squares) and a noninteracting sample (circles). Parameters: $p=30\%$ ($Co_{16}Cu_{84}$) and $T=82$ K. Coalescence is allowed in both samples.

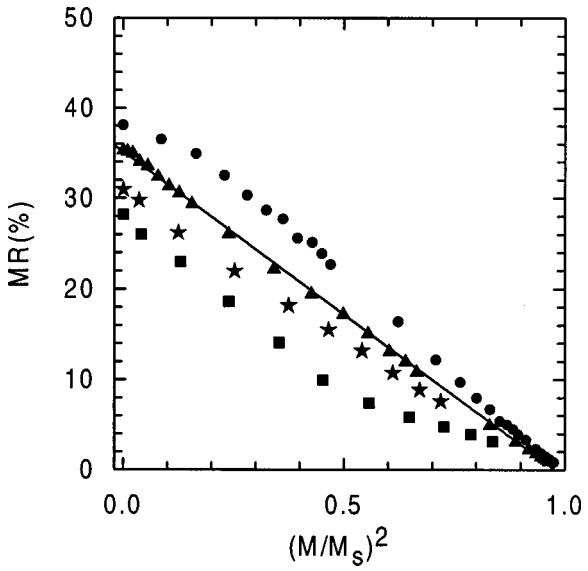

FIG. 13. Anhysteretic magnetoresistance versus reduced magnetization. Data for a monodisperse noninteracting system (triangles), a monodisperse dipolar system (stars), a polydisperse noninteracting system (circles), and a polydisperse dipolar system (squares) are shown. The monodisperse samples have $V=3$ and the polydisperse samples have $\langle V\rangle\sim 3.06$. (The volume of a monomer is defined as the volume unit). Parameters: $p=30\%$($Co_{16}Cu_{84}$) and $T=82$ K.

switched on, a reduction of the MR values is observed, which is, however, more dramatic in the polydisperse than the monodisperse sample. In other words, dipolar interactions cause a stronger reduction of the GMR effect as the width of the size distribution increases. This trend was also observed in the experimental data of Allia *et al.*,[10] where the largest reductions of the MR values due to dipolar interactions were observed in the sample $Co_{15}Cu_{85}$, in which the size distribution was nearly flat, and consequently all cluster sizes were equally probable. On the contrary for the sample $Co_{15}Cu_{85}$, that was nearly monodisperse, a weak flattening ($\sim$10%) of the MR curve was measured. An explanation for this behavior is that in the polydisperse sample, the large clusters ($V>3$) produce strong magnetostatic fields that cause an efficient alignment of the surrounding small clusters ($V<3$), thus large positive correlations are introduced in the magnetic structure that lead to a severe reduction of the MR.

Regarding the shape of the curves in Fig. 13 we notice that the data for the monodisperse noninteracting sample fit on a straight line over the whole range of magnetization, but this is not the case for the noninteracting polydisperse sample. When a weak field is applied to a noninteracting polydisperse sample, the larger clusters are aligned along the field while the smaller ones are not due to thermal fluctuations. This differentiation in the response of the various clusters to the applied field leads to the deviations from the straight line fit close to zero magnetization. When the dipolar interactions are present, deviations from a parabolic dependence occur, which are more severe for the polydisperse system.

Ferrari *et al.*[8] have shown that the effect of size distribution on the MR values is best observed if the normalized magnetoresistance, defined as $MR_n=MR/MR_{max}$, is plotted as a function of the sample magnetization. For a noninteract-

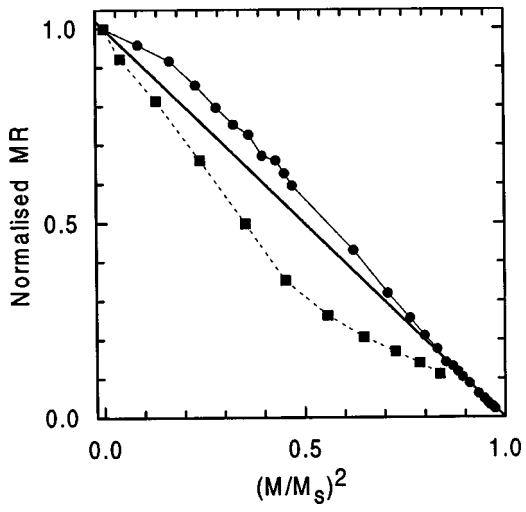

FIG. 14. Normalized anhysteretic magnetoresistance versus reduced magnetization for a dipolar sample (squares) and for a noninteracting sample (circles). Parameters: $p=30\%$ ($Co_{16}Cu_{84}$) and $T=82$ K. Coalescence is allowed in both samples.

ing monodisperse sample, under the assumption that the resistance is a quadratic function of the sample magnetization [22] and using the above definition of MR (Ref. 33) we obtain the parabolic law $MR_n=1-(M/M_s)^2$. Ferrari *et al.*, using the transport model of Zhang and Levy,[16] showed that when a size distribution exists in the sample, the MR_n curve lies above the $1-(M/M_s)^2$ parabola. Our data in Fig. 14 reproduce this behavior for the noninteracting sample with a cluster size distribution. Interestingly, when dipolar interactions are present a qualitative difference is observed, as the MR_n curve lies below the reference parabola. This result suggests that the plots of the MR_n vs M/M_s provide information on the relative importance of the interaction effects.

IV. CONCLUSIONS

We have developed a theoretical scheme appropriate to study the giant magnetoresistance effect in granular metal films, that includes the effect of grain size distribution and magnetostatic interactions between the grains. The scheme combines the Monte Carlo simulation, that provides a realistic description of the micromagnetic structure and the Kubo formula for the conductivity, which is valid in the whole concentration range. We have assumed spin-dependent scattering to be the cause of the GMR effect and we have described the electronic structure of the granular alloy by a tight binding Hamiltonian with a single spin-polarized band.

We have calculated the concentration dependence of the MR for a Co_xCu_{1-x} alloy over the whole range of concentrations ($0\leqslant x\leqslant 1$) taking into account the effect of cluster formation due to magnetic particle coalescence. We have found an optimum MR value around the percolation threshold, in agreement with experiments. We have demonstrated that close to the percolation threshold, the dipolar interactions among the clusters cause the largest reduction of the MR values and thus they seriously modify the optimum MR value. We have attributed this behavior to the presence of a wide distribution of cluster sizes in the system and a corresponding wide distribution of local fields. Multidomain formation in large clusters, whose size exceeds the exchange correlation length (typically a few hundreds Å) occurs in dense samples. This effect is expected to reduce the role of dipolar interactions between clusters and also modify the concentration dependence of MR. The cases studied within our present model, namely, the case of well separated particles and that of fully saturated clusters, constitute the two extreme limits as regards the role of the dipolar interactions. We expect a smooth transition between the results in these two limiting cases as the saturation condition within the clusters is gradually relaxed and magnetic domains form.

Finally, we have investigated the combined effects of dipolar interactions and cluster size distribution on the MR of a granular Co_xCu_{1-x} system below the percolation threshold. We obtained deviations from the MR vs (M/Ms) parabola at low fields in agreement with experiments on polydisperse samples. Magnetostatic interactions and particle size dispersion have opposite effects on the MR value of the granular alloy. Size dispersion alone causes enhancement of the MR, while interactions always have a degrading effect. Most interestingly, the effect of dipolar interactions is amplified in the presence of a wide distribution of cluster sizes. By examination of the normalized MR curves, we found that size distribution and interaction effects produce deviations from the theoretical $1-M^2$ line in opposite directions. We therefore suggest that the normalized MR curves provide an indication of the relative importance of interaction effects.

ACKNOWLEDGMENTS

We would like to thank Professor R. J. Elliott for many valuable discussions during the course of this work. This work was financially supported by the program Demoerevna 99 (Program No. 638).

[1] A. E. Berkowitz, J. R. Mitchell, M. J. Carey, A. P. Young, S. Zhang, F. E. Spada, F. T. Parker, A. Hutten, and G. Thomas, Phys. Rev. Lett. **68**, 3745 (1992).

[2] J. Q. Xiao, J. S. Jiang, and C. L. Chien, Phys. Rev. Lett. **68**, 3749 (1992).

[3] M. N. Baibich, J. M. Broto, A. Fert, F. Nguyen van Dau, F. Petroff, P. Etienne, G. Creuzet, A. Friederich, and J. Gazeles, Phys. Rev. Lett. **61**, 2472 (1988).

[4] C. Vouille, A. Barthélémy, F. Elokan Mpondo, A. Fert, P. A. Schroeder, S. Y. Hsu, A. Reily, and R. Loloee, Phys. Rev. B **60**, 6710 (1999).

[5] W. P. Pratt, Jr., S. F. Lee, J. M. Slaughter, R. Loloee, P. A. Schroeder, and J. Bass, Phys. Rev. Lett. **66**, 3060 (1991).

[6] F. Parent, J. Tuaillon, L. B. Stern, V. Dupuis, B. Prevel, A. Perez, P. Melinon, G. Guiraud, R. Morel, A. Barthelemy, and A. Fert, Phys. Rev. B **55**, 3683 (1997).

[7] M. M. Pereira de Alzevedo, G. N. Kakazei, A. F. Kravetz, V. S. Amaral, Yu. G. Pogorelov, and J. B. Sousa, J. Magn. Magn. Mater. **196–197**, 40 (1999).

[8] E. F. Ferrari, F. C. S. da Silva, and M. Knobel, Phys. Rev. B **56**,

6086 (1997).
[9] A. Fert and P. Bruno, in *Ultrathin Magnetic Structure II*, edited by B. Heinrich and J. A. C. Bland (Springer Verlag, Berlin, 1994), p. 82.
[10] P. Allia, M. Knobel, P. Tiberto, and F. Vinai, Phys. Rev. B **52**, 15 398 (1995).
[11] B. J. Hickey, M. A. Howson, S. O. Musa, and N. Wiser, Phys. Rev. B **51**, 667 (1995).
[12] J. F. Gregg, S. M. Thompson, S. J. Dawson, K. Ounadjela, C. R. Staddon, J. Hamman, C. Fermon, G. Saux, and K. O'Grady, Phys. Rev. B **49**, 1064 (1994).
[13] M. Rubinstein, Phys. Rev. B **50**, 3830 (1994).
[14] R. Y. Gu, L. Sheng, D. Y. Xing, Z. D. Wang, and J. M. Dong, Phys. Rev. B **53**, 11 685 (1996).
[15] E. F. Ferrari, F. C. S. da Silva, and M. Knobel, Phys. Rev. B **59**, 8412 (1999).
[16] S. Zhang and P. M. Levy, J. Appl. Phys. **73**, 5315 (1993).
[17] L. Xing and Y.-C. Chang, Phys. Rev. B **48**, 4156 (1993).
[18] Y. G. Pogorelov, M. M. P. de Azevedo, and J. B. Sousa, Phys. Rev. B **58**, 425 (1998).
[19] Y. Asano, A. Oguri, J. Inoue, and S. Maekawa, Phys. Rev. B **49**, 12 831 (1994).
[20] A. Vedyayev, B. Mevel, N. Ryzhanova, M. Tsiev, B. Dieny, A. Chamberod, and F. Brouers, J. Magn. Magn. Mater. **164**, 91 (1996).
[21] D. Kechrakos and K. N. Trohidou, Phys. Rev. B **58**, 12 169 (1998).
[22] J. I. Gittleman, Y. Goldstein, and S. Bozowski, Phys. Rev. B **9**, 3609 (1972).
[23] M. El'Hilo, R. W. Chantrell, and K. O'Grady, J. Appl. Phys. **84**, 5114 (1998).
[24] D. Altbir, P. Vargas, J. d' Albuquerque e Castro, and U. Raff, Phys. Rev. B **57**, 13 604 (1998).
[25] D. Kechrakos and K. N. Trohidou, J. Appl. Phys. **87**, 5179 (2000).
[26] E. Y. Tsymbal and D. G. Pettifor, Phys. Rev. B **54**, 15 314 (1996).
[27] E. Y. Tsymbal, D. G. Pettifor, J. Shi, and M. B. Salamon, Phys. Rev. B **59**, 8371 (1999).
[28] Y. Asano, A. Oguri, J. Inoue, and S. Maekawa, J. Magn. Magn. Mater. **140–144**, 505 (1995).
[29] D. Stauffer, *Introduction to Percolation Theory* (Taylor & Francis, London, 1985).
[30] S. H. Baker, S. C. Thornton, A. M. Keen, T. I. Preston, C. Norris, K. W. Edmonds, and C. Binns, Rev. Sci. Instrum. **68**, 1853 (1997).
[31] M. P. Lopez-Sancho, J. M. Lopez-Sancho, and J. Rubio, J. Phys. F: Met. Phys. **14**, 1205 (1984).
[32] K. Binder and D. W. Heermann, *Monte Carlo Simulation in Statistical Physics*, Vol. 80 of Springer Series in Solid-State Sciences (Springer Verlag, Berlin, 1998).
[33] S. S. P. Parkin, N. More, and K. P. Roche, Phys. Rev. Lett. **64**, 2304 (1990).
[34] J. M. Luttinger and L. Tisza, Phys. Rev. **70**, 954 (1946).